

The distance modulus determined from Carmeli's cosmology fits the accelerating universe data of the high-redshift type Ia supernovae without dark matter

John G. Hartnett*

*School of Physics, the University of Western Australia
35 Stirling Hwy, Crawley 6009 WA Australia*

(Dated: October 13, 2019)

The velocity of the Hubble expansion has been added to General Relativity by Moshe Carmeli and this resulted in new equations of motion for the expanding universe. A new relationship between the distance and supernova redshift is found that fits the magnitude-redshift data of the high-z supernova teams without the need for the inclusion of dark matter. This result confirms that universe is accelerating, asymptotically expanding towards a spatially flat state. Best fits to the data indicate that the vacuum energy density Ω_Λ and the (baryonic) matter density Ω_m sum to a total $\Omega_\Lambda + \Omega_m = 1.029$ in the present universe. The theory applied to the data also clearly distinguishes that the expansion is speed-limited. That is, from the two models applied, one Doppler speed limited and the other not, the speed limited model was a vastly better fit.

PACS numbers: 95.30.Sf 95.35.+d 98.62.Py 98.80.Es

I. INTRODUCTION

The metric [1, 6] used by Carmeli in a generally covariant theory (Cosmological General Relativity) extends the number of dimensions of the universe by the addition of a new dimension – the radial velocity of the galaxies in the Hubble flow. The Hubble law is assumed as a fundamental axiom for the universe and the galaxies are distributed accordingly.

In determining the large scale structure of the universe the usual time dimension is neglected as observations are taken over such a short time period compared to the motion of the galaxies in the expansion. In this case, the usual time coordinate (t) does not need to be considered. This leaves only four dimensions to be considered – three of space and one of velocity. In general, however, the new 5D cosmology developed by Carmeli contains all of general relativity as a subset. All of the results in general relativity that are experimentally supported are also obtained in Cosmological General Relativity (CGR) [7].

When discussing the motions of stars and gases in galaxies the five dimensional cosmology must be used. Both the usual geodesic equation and a new phase space equation have been derived using CGR. From this Carmeli was able to derive a Tully-Fisher like equation [5], which indicates that the existence of halo dark matter is not necessary to be assumed in spiral galaxies.

II. COSMOLOGICAL GENERAL RELATIVITY

Here the CGR theory is considered using a Riemannian four-dimensional presentation of gravitation in which the

coordinates are those of Hubble, i.e. distance and velocity, or more precisely, proper distances as measured by the Hubble law and the measured redshifts of galaxies. This results in a phase space equation where the observables are redshift and distance. The latter may be determined from the high-redshift type Ia supernovae (SNe Ia) observations.

A. Line element

In the case considered here the line element is

$$ds^2 = \tau^2 dv^2 - e^\xi dr^2 - R^2(d\theta^2 + \sin^2\theta d\phi^2) \quad (1)$$

where $dr^2 = (dx^1)^2 + (dx^2)^2 + (dx^3)^2$, ξ and R are functions of v and r alone and comoving co-ordinates $x^\mu = (x^0, x^1, x^2, x^3) = (\tau v, r, \theta, \phi)$ are used. The new dimension (v) is the radial velocity of the galaxies in the expanding universe, and is not the time derivative of the distance. The parameter τ , the Hubble-Carmeli time constant, is a constant at any epoch and its reciprocal (designated h) is the Hubble 'constant' measured in the limit of zero distance and zero gravity, which is only approximately the Hubble constant H_0 .

Equation (1) then represents a curved *spacevelocity* which, like in general relativity, may be represented by a four-dimensional Riemannian manifold with a metric $g_{\mu\nu}$ and a line element $ds^2 = g_{\mu\nu}dx^\mu dx^\nu$. This differs from general relativity in that here the x^0 coordinate is velocity-like instead of time-like as is the case of $x^0 = ct$, where c is the speed of light and a universal constant. The parameter t is the time coordinate. In this theory $x^0 = \tau v$, where τ is also a universal constant. The other three coordinates x^k , $k = 1, 2, 3$, are space-like, as in general relativity.

The line element represents a spherically symmetric isotropic universe, and the expansion is the result of the

*Electronic address: john@physics.uwa.edu.au

Hubble expansion. The expansion is observed at a definite time and therefore as mentioned above, $dt = 0$. Using spherical spatial coordinates (r, θ, ϕ) and taking into account $d\theta = d\phi = 0$ (the isotropy condition) then dr represents the radial co-ordinate distance to the source.

The universe expansion is obtained from (1) as a null condition, i.e. $ds = 0$. The null condition in the limit of no matter or gravity (i.e. $e^\xi = 1$) then yields $dr/dv = \pm\tau$, which when integrated with appropriate initial conditions results in $r = \tau v$ in an expanding universe. This can be rewritten as $v = hr \approx H_0 r$, the Hubble law in the zero-gravity limit. And because the Hubble law is assumed (i.e. the redshifts are inherently the result of expansion) the distances are the proper distances to their sources.

B. Field equations

In CGR, as in general relativity, one equates geometry to physics. In this theory Einstein's field equations

$$G_{\mu\nu} = R_{\mu\nu} - \frac{1}{2}g_{\mu\nu}R = \kappa T_{\mu\nu} \quad (2)$$

are modified.

The energy-momentum tensor $(T_{\mu\nu})$ takes on a different physical meaning. The coupling constant (κ) that relates the geometry $G_{\mu\nu}$ in (2) to the energy terms $T_{\mu\nu}$ is also different. However the form of (2) is exactly the same as in general relativity, but with $\kappa = 8\pi k/\tau^4$ and $k = G\tau^2/c^2$ where G is Newton's gravitational constant. Therefore $\kappa = 8\pi G/c^2\tau^2$.

The correspondence with general relativity is easily seen by the substitutions $c \rightarrow \tau$ and $t \rightarrow v$. In this new theory the energy-momentum tensor $T^{\mu\nu}$ is constructed with these substitutions. As usual $T^{\mu\nu} = \rho u^\mu u^\nu$, where ρ is the average mass/energy density of the universe and $u^\mu = dx^\mu/ds$ is the four-velocity.

In general relativity $T_0^0 = \rho$. In Newtonian gravity the potential function is defined by the Poisson equation $\nabla^2\phi = 4\pi G\rho$. Where $\rho = 0$ the vacuum Einstein field equations are usually solved in general relativity and similarly Laplace's equation in the Newtonian theory.

These are valid solutions but in cosmology there never exists the situation where the density ρ is zero because the universe always contains matter and/or energy. So in order to equate the rhs of (2) to zero Carmeli took $T_0^0 \neq \rho$ but $T_0^0 = \rho_{eff} = \rho - \rho_c$, in the appropriate units. Here ρ_c is the critical or "closure" density and in this model

$$\rho_c = \frac{3}{8\pi G\tau^2} \approx 10^{-29} \text{ g.cm}^{-3}.$$

Therefore in CGR $T^{\mu\nu} = \rho_{eff}u^\mu u^\nu$.

The result is that we can view the universe, in *spacevelocity*, or phase space as being stress free when the matter density of the universe is equal to the critical density.

That is, $\rho_{eff} = 0$. This then gives us the analogous situation to that in the Newtonian and Einsteinian theories. Besides the assumption of the universality of the Hubble Law, this is the second fundamental assumption in this cosmology.

C. Phase space equation

In *spacevelocity* the null condition $ds = 0$ describes the expansion of the universe. Therefore it follows from (1) for a spherically symmetric distribution of matter

$$\tau^2 dv^2 - e^\xi dr^2 = 0 \quad (3)$$

which results in

$$\frac{dr}{dv} = \pm\tau e^{-\xi/2}. \quad (4)$$

The positive sign is chosen for an expanding universe.

Equation (4) has been solved in [6, 7]. Because r , θ and ϕ are constants along the geodesics for the above chosen co-ordinates $dx^0 = ds$ and therefore $u^\alpha = u_\alpha = (1, 0, 0, 0)$. Using this and equation (2) written as

$$R_{\mu\nu} = \kappa(T_{\mu\nu} - \frac{1}{2}g_{\mu\nu}T) \quad (5)$$

where $T = T_{\mu\nu}g^{\mu\nu}$ and

$$T_{\mu\nu} = \rho_{eff}u_\mu u_\nu + p(u_\mu u_\nu - g_{\mu\nu}) \quad (6)$$

where p is the pressure, one finds that the only non-vanishing components of $T_{\mu\nu}$ are $T_{00} = \tau^2\rho_{eff}$, $T_{11} = pe^\xi\tau/c$, $T_{22} = pR^2\tau/c$, $T_{33} = pR^2\sin^2\theta\tau/c$ and $T = \tau^2\rho_{eff} - 3p\tau/c$.

After some manipulation there remains only three independent field equations [7], which are reproduced here.

$$e^\xi(2R\ddot{R} + \dot{R}^2 + 1) - R'^2 = -\kappa e^\xi R^2 p\tau/c \quad (7)$$

$$2\dot{R}' - R'\dot{\xi} = 0 \quad (8)$$

$$\begin{aligned} e^{-\xi} \left[\frac{R'}{R} \xi' - \left(\frac{R'}{R} \right)^2 - 2\frac{R''}{R} \right] + \frac{\dot{R}}{R} \dot{\xi} \\ + \left(\frac{\dot{R}}{R} \right)^2 + \frac{1}{R^2} = \kappa\tau^2\rho_{eff} \end{aligned} \quad (9)$$

where the dots and primes denote differentiation with respect to v and r respectively.

D. Solution to field equations

Carmeli found a solution to equation (8), with the necessary condition that $R' > 0$, as

$$R = r \quad (10)$$

and

$$e^\xi = \frac{1}{1 + f(r)} \quad (11)$$

where $f(r)$ is an arbitrary function of r and satisfies $f(r) + 1 > 0$. Substituting (10) into (7) and (9) it can be shown, using $\kappa = 8\pi G/c^2\tau^2$ and $\rho_c = 3/8\pi G\tau^2$ that

$$f(r) = \frac{1 - \Omega}{c^2\tau^2} r^2, \quad (12)$$

where $\Omega = \rho/\rho_c$. This is the density at the epoch defined by the distance r . By substituting (11) with (12) into (4) we get Carmeli's solution

$$\frac{dr}{dv} = \tau \sqrt{1 + (1 - \Omega) \frac{r^2}{c^2\tau^2}}, \quad (13)$$

where the positive solution has been chosen for an expanding universe.

Equation (13) may be integrated exactly to get

$$r(v) = \frac{c\tau}{\sqrt{1 - \Omega}} \sinh\left(\frac{v}{c}\sqrt{1 - \Omega}\right) \quad \forall \Omega. \quad (14)$$

Thus (14) may be written in terms of normalized or natural units $r/c\tau$ and for arbitrary $z = v/c$,

$$\frac{r}{c\tau} = \frac{\sinh(z\sqrt{1 - \Omega})}{\sqrt{1 - \Omega}}. \quad (15)$$

Considering the expansion of the universe it is clear that (15) describes a tri-phase expansion. Initially the universe is very dense and $\Omega > 1$ so the hyperbolic sine function becomes a normal trigonometric sine function describing a decelerating expansion. Then the density Ω reaches unity and the rhs of (15) becomes equal to z which describes a coasting stage. Finally the density decreases and $\Omega < 1$ as the universe continues to expand. Then the hyperbolic sine function represents an exponentially accelerating universe.

III. MATTER DENSITY VERSUS REDSHIFT

Now let us consider what happens to the density of matter as we look back in the cosmos as a function of redshift, z . Carmeli assumed that the value of Ω in (15) is fixed and plotted curves as functions of redshift for various values of Ω . (See figure A4, on page 134 of [6].)

In 1996 Carmeli predicted that the universe must be accelerating [4]. He predicted the form of the high redshift data of Riess *et al* [19], published in 1998, which

announced an accelerating universe following the observations of Garnavich *et al* [11] and Perlmutter *et al* [17]. Therefore in 1998, Carmeli assumed a value of total matter (normal baryonic matter + dark matter) density $\Omega = 0.245$, which was the accepted value then for what we will designate Ω_m the density at the present epoch. However, more correctly Ω varies as a function of redshift, z .

A. Baryonic matter density

The density of normal baryonic matter in the universe has generally come from considerations of big bang nucleosynthesis (BBN)[15] [16]. The predicted primordial abundance of the light elements are assumed to have been produced in the big bang and not in stars. Hence a comparison between predicted abundances and abundances inferred from observed baryon-to-photon ratios are used to put an upper limit on the baryon density.

Deuterium is believed to be only destroyed by stellar processing, therefore any observation of its interstellar or solar system abundance would put a lower bound on its primordial abundance since it is believed that it was all created in the BBN process.

As a result a lower bound on deuterium translates into a so-called 'robust' upper bound on the density of baryons. Following this line of logic the observed interstellar value of $D/H \geq (1.6 \pm 0.2) \times 10^{-5}$ puts a limit on the baryon density $\Omega_b h^2 \leq 0.027(2\sigma)$ [15]. An earlier determination produced $\Omega_b h^2 \leq 0.015 \pm 0.005$ [16]. (Here Ω_b is the baryonic density expressed as a fraction of the critical density and h is the Hubble constant as a fraction of $100 \text{ km.s}^{-1} \text{Mpc}^{-1}$ and not to be confused with $h = 1/\tau$ used in this paper.) Assuming a value of the Hubble parameter $h = 0.7$ these two sources put $\Omega_m \leq 0.055$ and ≤ 0.031 respectively.

Two comments may be made. Firstly, the standard model and the BBN process are assumed to determine the matter density at the current epoch. Part of the underlying assumption resides with the success of the standard model to predict the measured helium abundance (${}^4\text{He}/H$) and the existence of the cosmic microwave background radiation. But this line of reasoning would only hold true if there was no other way to explain these observations.

The second comment is in regard to the assumption that all the light elements including deuterium and helium are primordial via the BBN process. If it could be shown that there are other genesis processes, in fact, that these nuclides could be manufactured in stars then this reasoning would break down. Such suggestions have been made [3].

A process described by Burbidge *et al* [2] now called B^2FH after the authors successfully showed nearly all nuclides could be generated in stars. Now Burbidge and Hoyle [3] contend that all helium is created in stars and the energy released ($4.37 \times 10^{-13} \text{ ergs.cm}^{-3}$) is almost

exactly equal to the energy contained in the cosmic microwave background. They further contend when this energy is thermalised the resulting temperature is $2.76K$, also that the synthesis of the other light elements occurs in stars and observational evidence is cited therein.

Nevertheless the aforementioned values of Ω_b agree well with the locally measured baryonic budget. One study yields a range $0.007 \leq \Omega_b \leq 0.041$ at $z \approx 0$ with a best guess of $\Omega_b \approx 0.021$ where a Hubble constant of $70 \text{ km.s}^{-1}\text{Mpc}^{-1}$ was assumed [10].

Now, determinations of the total matter density (including dark matter), at high redshifts, have been made, for example, from X-ray measurements of the gas content in galaxy clusters combined with the total virial masses [22]. The calculation of the virial masses in turn assumes that the equations describing the motions of the constituents in the clusters are correct.

However it is well-known that mass-to-light ratios vary over all mass scales from galaxies to superclusters [23]. This may be the result of an incorrect understanding of the physics which has resulted in incorrect dynamical masses. That conclusion is suggested by Carmeli's derivation of a Tully-Fisher type relation for galaxies [5] and by a new post-Newtonian equation describing the dynamics of the stars and gases in spiral galaxies [12]. The latter produces the galaxy rotation curves that have been used as evidence for halo dark matter. Using the Carmeli model no halo dark matter is necessary to be assumed.

The question then remains. Do the high- z SNe Ia data fit this model without the need to assume the existence of dark matter? If so, then the issues can be addressed to explain the much higher than expected dynamical masses of clusters etc at high redshift.

B. Matter density at the present epoch

This paper makes no determinations about the matter density, dark, baryonic or otherwise at high redshift except the following, with a justification in section VI.

$$\Omega = \Omega_m(1+z)^3, \quad (16)$$

where Ω_m is then the averaged matter density, at the present epoch, expressed as a fraction of the critical or "closure" density. Equation (16) results from the fact that as the redshift increases the volume decreases as $(1+z)^3$.

The value of the baryonic matter density commonly cited is $\rho = 3 \times 10^{-31} \text{ g.cm}^{-3}$. Here this is assumed to be the total matter density and therefore, expressed as a fraction of the critical density, $\Omega_m \approx 0.03$ in (16).

Substituting (16) into (15) we get

$$\frac{r}{c\tau} = \frac{\sinh(z\sqrt{1-\Omega_m(1+z)^3})}{\sqrt{1-\Omega_m(1+z)^3}}. \quad (17)$$

It has been shown [13] that (15) with $\Omega = 0.245$ (which Carmeli initially assumed) and (17) with $\Omega_m = 0.03$ are practically identical over the redshift range $0 < z < 1$. The difference between the two equations over the domain of the measurements is much less significant than the fit to the data. In fact, a local matter density of only $0.03 \leq \Omega_m \leq 0.04$ is necessary to have agreement. Once it is shown that this model fits the observational data it follows that this effectively eliminates the need for the existence of dark matter on the cosmic scale.

IV. COMPARISON WITH HIGH- z TYPE IA SUPERNOVAE DATA

In order to compare (17) with the data from the high redshift SNe Ia teams the proper distance is converted to magnitude as follows.

$$m(z) = \mathcal{M} + 5\log\mathcal{D}_L(z; \Omega), \quad (18)$$

where \mathcal{D}_L is the "Hubble constant free" luminosity distance. \mathcal{D}_L is related by

$$\mathcal{D}_L(z; \Omega) = (1+z)\frac{r}{c\tau} \quad (19)$$

using (17) and

$$\mathcal{M} = 5\log(c\tau) + 25 + M_B + a. \quad (20)$$

Here \mathcal{M} incorporates the various parameters that are independent of the redshift, z . The parameter M_B is the absolute magnitude of the supernova at the peak of its light-curve and the parameter a allows for any uncompensated extinction or offset in the mean of absolute magnitudes. The absolute magnitude then acts as a "standard candle" from which the luminosity and hence distance can be estimated.

The value of M_B need not be known, neither any other component in \mathcal{M} , as \mathcal{M} has the effect of merely shifting the fit curve (19) along the vertical magnitude axis.

By choosing the value of $\tau = 4.211 \times 10^{17} \text{ s} = 13.35 \text{ Gyr}$, which is the reciprocal of the chosen value of the Hubble constant in the gravity free limit $h = 73.27 \text{ km.s}^{-1}\text{Mpc}^{-1}$ (see section VI) $\mathcal{M} = 43.0595 + M_B + a$. In practice, where the distance modulus $(m - M_B)$ is used in the curve fits, a is a free parameter.

It has been one of the goals of cosmology to determine if the Hubble expansion is speed limited. That is, to answer the question of whether the cosmological expansion is governed by the relativistic Doppler effect or not. If it isn't then in (17) $v/c = z$, but if it is then as v approaches c it is necessary to replace v/c with $v/c = ((1+z)^2 - 1)/((1+z)^2 + 1)$. So by fitting to the data of the high- z SNe Ia it is possible to test this experimentally.

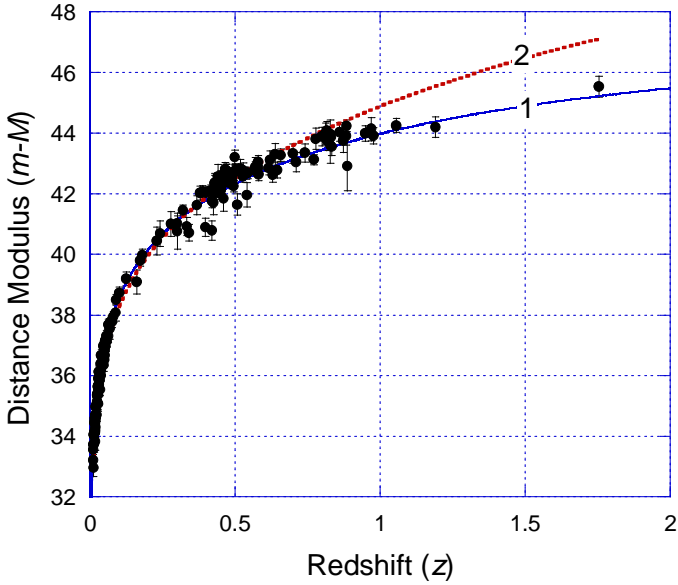


FIG. 1: (Color online) Data taken from Table 5 of Riess *et al.* Curve 1 (purple solid line) is the best fit and represents the speed limited model. Curve 2 (orange dots) is the non speed limited model. Both curves use the same value of $\Omega_m = 0.02$. In order to make curve 2 pass through the highest data points the required mass density Ω_m must be larger than 0.10. However such values are unphysical

In figure 1 (18) has been plotted against the distance modulus ($m - M_B$) data taken from Table 5 of Riess *et al* [20]. Curve 1 is the best fit to the data using (17) with $v/c = ((1+z)^2 - 1)/((1+z)^2 + 1)$, the speed limited model and curve 2 is (17) with $v/c = z$ the non speed limited model. This immediately answers the question, the Hubble expansion as seen from our position as observer is speed limited, by the usual relativistic effect.

It can be seen that curve 2 departs from curve 1 slightly above redshift, $z = 0.5$. Both curves have been plotted with a value of $\Omega_m = 0.02$, which is the best fit for curve 1. However different ‘best fit’ offsets (a) have resulted. The parameter, a , was used as a free parameter. For curve 1, $a = 0.4098$ and for curve 2, $a = 0.0105$. There are a total of $N = 163$ data and the residual for the speed limited version of (17) is $R = 0.9960$, with $\chi^2 = 17.638$ and hence $\chi^2/N = 0.1082$. The residual for the non speed limited version of (17) is $R = 0.9935$, with $\chi^2 = 28.537$ and hence $\chi^2/N = 0.1751$.

In order to make curve 2 pass through the highest data points the requirement on the mass density is $\Omega_m \geq 0.10$, which is unphysical. As mentioned III B, the local baryonic matter budget has been measured in the range $0.007 \leq \Omega_m \leq 0.041$ [10] with a best guess of $\Omega_m \approx 0.021$. The latter is consistent with the best fit from this data set. Therefore, in the following analysis, only the speed-

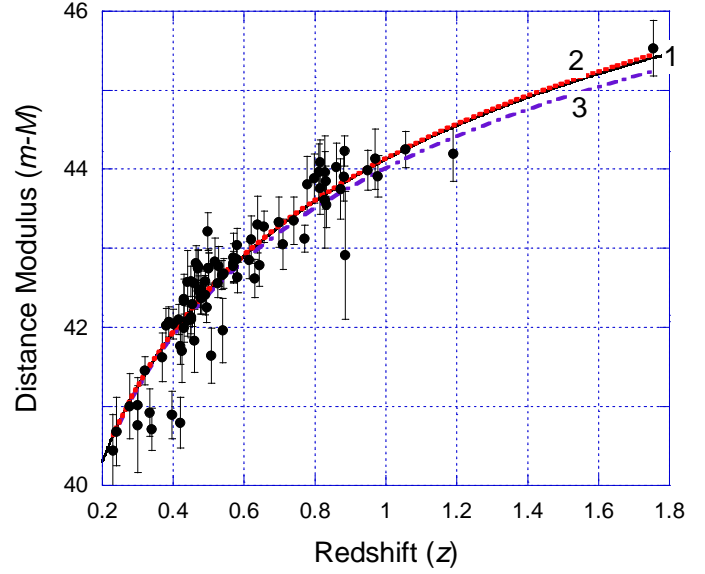


FIG. 2: (Color online) Data taken from Riess *et al* for $z > 0.2$. Curve 1 (black solid line) is the best fit and represents (18) with the speed-limited (21). Curve 2 (orange dots) represents (18) with $\Omega = \Omega_m = 0$ and curve 3 (purple dot dash) represents (18) with $\Omega = 1$

limited form of (17) will be used, that is

$$\frac{r}{c\tau} = \frac{\sinh(\varsigma \sqrt{1 - \Omega_m(1+z)^3})}{\sqrt{1 - \Omega_m(1+z)^3}} \quad (21)$$

where $\varsigma = ((1+z)^2 - 1)/((1+z)^2 + 1)$.

Figure 2 shows the data of figure 1 but for $z > 0.2$. Curve 1 (solid line) is the best fit curve over the range of the selected data and consistent with measured values i.e. $\Omega_m \geq 0.007$. Instead of $\Omega_m = 0.02$, the best fit curve requires $\Omega_m = 0.0074 \pm 0.0507$ (statistical). However, the value of Ω_m may range up to 0.04 with little change in residuals. A slightly increased value of $a = 0.5312$ results compared with the fit in figure 1. This may indicate a small 0.12 additional extinction over the low redshift data. Here $N = 85$, the residual $R = 0.9344$, $\chi^2 = 10.513$ and hence $\chi^2/N = 0.1237$. Curve 2 (dots) represents (18) with $\Omega = \Omega_m = 0$ and curve 3 (dot dash) represents (18) with $\Omega = 1$. Curve 3 represents a universe where the matter density is always critical regardless of epoch.

Figure 3 shows the 8 new SNe Ia data from Tonry *et al* [21] for sources with $z > 0.2$. The resulting best fit is shown, with $\Omega_m = 0.0733 \pm 0.0978$ (statistical), $a = 0.5556$, the residual $R = 0.9938$, $\chi^2 = 0.1460$ and hence $\chi^2/N = 0.0183$. Tonry *et al* used 4 methods of analysis and averaged the results. The data shown in figure 3 is drawn from their Table 6, column 4.

Figure 4 shows 30 type SNe Ia data (which includes 11 new SNe) from Knop *et al* [14] for sources with $z > 0.2$. In this case the magnitude has been plotted against redshift. These data are taken from column 4 of Tables 3 and 4 in Knop *et al*. As with the other data various correc-

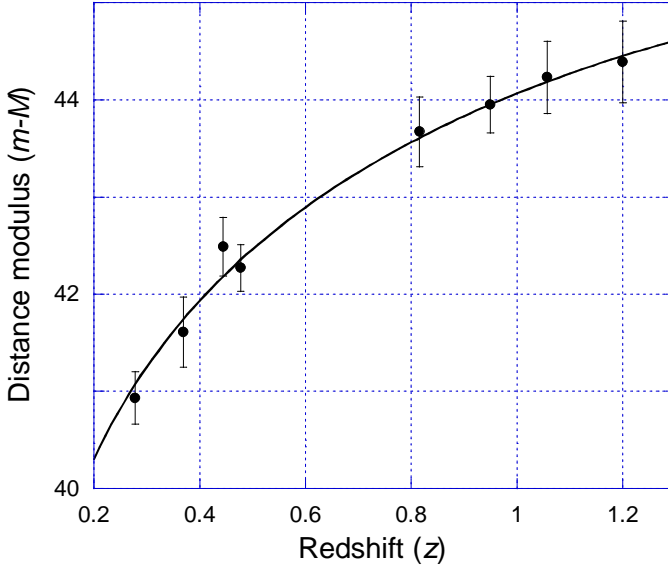


FIG. 3: Data taken from Tonry *et al.* The curve (solid line) is the best fit and represents (18) with the speed-limited (21)

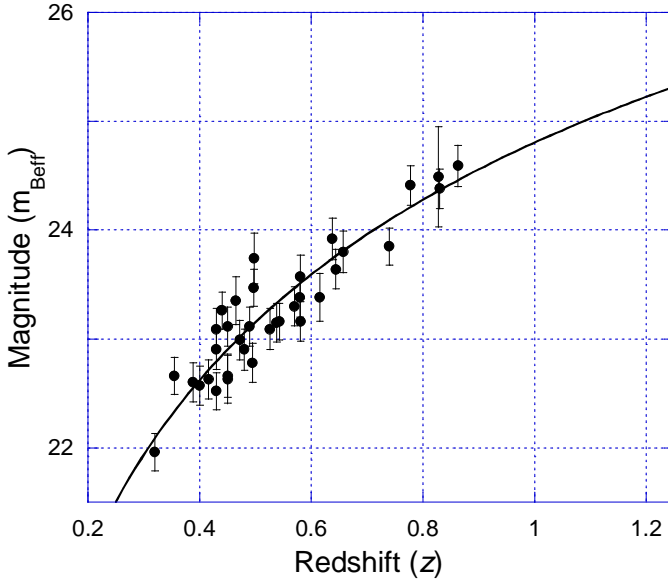


FIG. 4: Data taken from Knop *et al* for $z > 0.2$. The curve (solid line) is the best fit and represents (18) with the speed-limited (21)

tions have been applied, including K -correction, Galactic extinction, and light-curve stretch correction. (See references for details). In the figure 4 data, the host galaxy correction data (column 5 from (Knop *et al*) was not used at it added a large scatter to the data without significant improvement. The resulting best fit is shown, with $\Omega_m = 0.0193 \pm 0.1374$ (statistical), the residual $R = 0.9217$, $\chi^2 = 1.9323$ and hence $\chi^2/N = 0.0644$. Because effective apparent magnitude $m_{B\text{eff}}$ was used instead of distance modulus the offset is $M_B + a = -18.760$.

Using this model it is clear from figure 2, that a lot

more and higher quality data are needed to test which density curve fits best. However from this analysis by taking the statistical average of the resulting Ω_m values from the high redshift data (figures 2 - 4), we get

$$\Omega_m = \sqrt{\sum_i w_i \Omega_{mi}^2} = 0.022 \pm 0.084, \quad (22)$$

where w_i is the weighting fraction of data in the fits, and Ω_{mi} are the best fit values from the three data sets used.

V. CURVED SPACEVELOCITY

In section III B on matter density it was assumed that the density could be described by the function in (16) that assumes the universe is essentially spatially Euclidean. This assumption is justified in section VII. However it is obvious that besides locally, i.e. for small z and for the condition where $\Omega = 1$, *spacevelocity* is not flat in general and is expected to modify the expression in (16). When $\Omega > 1$ it is curved and closed and when $\Omega < 1$ it is curved and open. Equation (16) relates the density to the value (Ω_m) in Euclidean space at the present.

Rewriting (4) in an expanding universe we get

$$\frac{1}{c\tau} \frac{dr}{dz} = e^{-\xi/2}. \quad (23)$$

The result is the gradient of the spatial co-ordinate r with respect to the redshift z , normalized by the Hubble length $c\tau$.

Therefore it is clear from (23) that $e^{\xi/2} = 1$ under those conditions which produce the Hubble law in the weak gravity limit or for flat *spacevelocity*. It can be seen from (11) and (12) that $e^{\xi/2} = 1$ when $\Omega = 1$. Therefore we can use $e^{\xi/2}$ to define the curvature of *spacevelocity* as a function of redshift z . Because the density scales as the inverse cube of the radial coordinate and since the radial coordinate scales differentially as $e^{-\xi/2}$, then $e^{3\xi/2}$ may be a good estimate of how the density scales with redshift z . See Appendix for a more rigorous approach. The more rigorous approach yields an integral that can only be approximated and results in a transcendental equation which cannot be used in the curve fits. Whereas the former approach results in an analytic function that can be used in the curve fits.

By combining (16) with (11) and (12) we can write

$$\Omega = \frac{\Omega_m (1+z)^3}{\left(1 + (1-\Omega) \left(\frac{r}{c\tau}\right)^2\right)^{3/2}}. \quad (24)$$

When $\Omega = 1$ in the denominator of (24) we recover (16). To get density Ω as a function of z we substitute $r/c\tau$

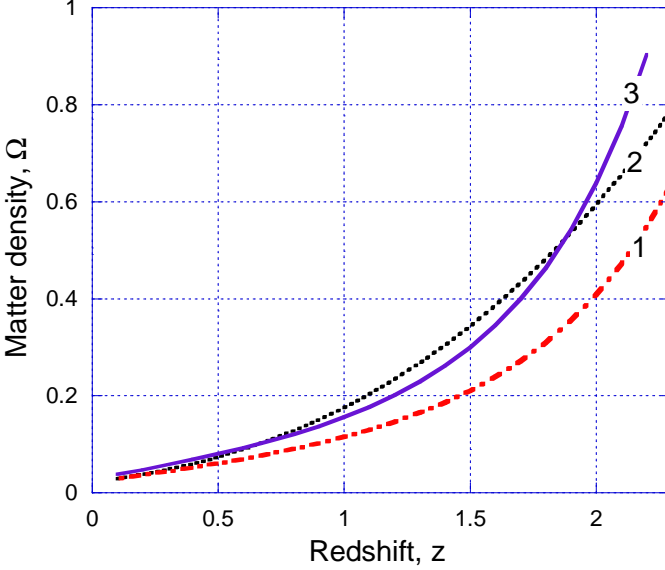


FIG. 5: (Color online) Matter density as a function of redshift z for the two models. Curve 1 (orange dot dash) is the flat *spacevelocity* density from (16) with $\Omega_m = 0.022$ taken from (22). The curved *spacevelocity* density from (25) with $\Omega_m = 0.022$ is represented by curve 2 (black dots), and with $\Omega_m = 0.029$ by curve 3 (purple solid line)

from (21).

$$\Omega = \frac{\Omega_m(1+z)^3}{\left(1 + \sinh^2\left(\zeta\sqrt{1-\Omega_m(1+z)^3}\right)\right)^{3/2}}, \quad (25)$$

where $\zeta = ((1+z)^2 - 1)/((1+z)^2 + 1)$.

This results in a new density function which is compared with (16) in figure 5. Curve 1 is the flat *spacevelocity* density from (16) with $\Omega_m = 0.022$ taken from (22). Curve 2 is for the curved *spacevelocity* density from (25) with the same value of $\Omega_m = 0.022$. Note the curves 1 and 2 are equivalent for $z < 0.4$. For small z we recover (16) from (25). Depending on the density Ω_m (25) is only valid over a limited range of z because of the condition $f(r) + 1 > 0$. For $\Omega_m = 0.022$ it is valid up to $z = 4.57$ and $\Omega_m = 0.029$ valid to $z = 4.11$.

The density from (25) is then substituted into (21) to get a new expression for $r/c\tau$ with only one free parameter Ω_m . This was then used in the same curve fits in section IV (figures 2 - 4) with the following results.

In each case the curve fits were improved by the new density model except for the figure 2 fit, which had a marginally worse χ^2 statistic. For the curve 1 of figure 1 the $\Omega_m = 0.02$ fit had a reduced $\chi^2 = 17.580$ but the same $R = 0.9960$. This resulted in a slight change in the offset $a = 0.4087$. For figure 2 the best fit $\Omega_m = 0.0133 \pm 0.0893$ (statistical) with offset $a = 0.56$ and residual $R = 0.9340$, $\chi^2 = 10.583$ and hence $\chi^2/N = 0.1245$. For figure 3 the best fit $\Omega_m = 0.0894 \pm 0.0645$ (statistical) with offset $a = 0.56$ and residual $R = 0.9939$, $\chi^2 = 0.1443$ and

hence $\chi^2/N = 0.0180$. For figure 4 the best fit $\Omega_m = 0.0289 \pm 0.1752$ (statistical) with offset $M_B + a = -18.76$ and residual $R = 0.9218$, $\chi^2 = 1.9317$ and hence $\chi^2/N = 0.0644$.

Finally by taking the weighted average as before

$$\Omega_m = \sqrt{\sum_i w_i \Omega_{mi}^2} = 0.029 \pm 0.115. \quad (26)$$

The new density function (25) has been plotted with $\Omega_m = 0.029$ in curve 3 in figure 5. Note curve 1 and 3 are essentially equal at small z except for the difference between initial Ω_m values, and only deviate from one another for $z > 0.66$. Initially curve 3 rises less steeply than curve 1 but for $z > 1.5$ it rises more strongly. Again the two density functions are equal at $z = 1.88$ for the values of Ω_m used in curves 1 and 3.

VI. HUBBLE PARAMETER

By inverting (21), multiplying both sides of the resulting equation by v/c and using the expression $v = H_0 r$ we get the following

$$H_0 = h \frac{\zeta \sqrt{1-\Omega}}{\sinh(\zeta \sqrt{1-\Omega})}. \quad (27)$$

with the density Ω taken from either (16) or (25).

As a result we have an expression which indicates that the Hubble parameter H_0 is scale length related and a function of the universal Hubble constant (h). It has been common to find figures cited in the literature that indicate ‘long’ and ‘short’ scales for H_0 . Studies with the Hubble Space Telescope using classical Cepheid variables yielded $H_0 = 80 \pm 17 \text{ km.s}^{-1}\text{Mpc}^{-1}$ [8] whereas studies using SN Ia yielded $H_0 = 67 \pm 7 \text{ km.s}^{-1}\text{Mpc}^{-1}$ [18]. See also [9].

It then follows from (27) that $h \approx 73.27 \text{ km.s}^{-1}\text{Mpc}^{-1}$ and $h \approx 73.51 \text{ km.s}^{-1}\text{Mpc}^{-1}$ respectively for $\Omega_m = 0.029$ or $\Omega_m = 0.022$ and the flat *spacevelocity* model (16) when a value of $H_0 = 70.00 \text{ km.s}^{-1}\text{Mpc}^{-1}$ at $z = 1$ is assumed. And $h \approx 73.60 \text{ km.s}^{-1}\text{Mpc}^{-1}$ for $\Omega_m = 0.029$ from (27) and the curved *spacevelocity* model (25). In any case, the specific value of h or its reciprocal τ cannot be determined from the data fit. An independent method must be used to determine the precise value of τ .

VII. DARK ENERGY

The vacuum or so-called ‘dark’ energy parameter Ω_Λ does not appear explicitly in Carmeli’s CGR. Hence the term ‘dark’ energy is a misnomer, and probably ‘vacuum’ energy is more correct. In any case, it is really a property of the metric. Only by a comparison with the standard

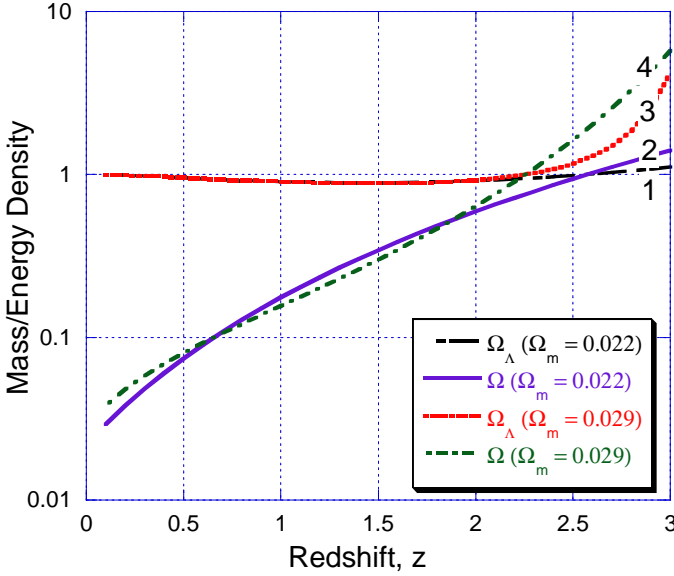


FIG. 6: (Color online) Ω_Λ and Ω as a function of redshift z for the two models. Curve 1 (black) and 2 (blue) are respectively Ω_Λ and Ω for the flat *spacevelocity* model with $\Omega_m = 0.022$. Curves 3 (red) and 4 (green) are respectively Ω_Λ and Ω for the curved *spacevelocity* model with $\Omega_m = 0.029$

Friedmann-Lemaitré-Robinson-Walker models can an assignment be made.

The vacuum energy density $\rho_\Lambda = \Lambda/8\pi G$ (in CGR) = $3H_0^2/8\pi G$ (from the standard theory). Also in CGR the critical density $\rho_c = 3h^2/8\pi G$. Therefore $\Omega_\Lambda = \rho_\Lambda/\rho_c = (H_0/h)^2$ and it follows from (27) that

$$\Omega_\Lambda = \left(\frac{\varsigma \sqrt{1-\Omega}}{\sinh(\varsigma \sqrt{1-\Omega})} \right)^2, \quad (28)$$

where the density Ω is taken from (16) and (25) and the resulting Ω_Λ , as a function of z , is shown in figure 6 for the two density models. Curve 1 and 2 are respectively the values of Ω_Λ and Ω for the flat *spacevelocity* model with $\Omega_m = 0.022$. Curve 3 and 4 are respectively the values of Ω_Λ and Ω for the curved *spacevelocity* model with $\Omega_m = 0.029$.

Figure 7 shows the values for the total energy density $\Omega + \Omega_\Lambda$ as a function of redshift, z . Curve 1 is for the flat *spacevelocity* model with $\Omega_m = 0.022$ and curve 2 is for the curved *spacevelocity* model with $\Omega_m = 0.029$.

For redshift $z < 2$ both models produce nearly the same total density. In both cases the total density $\Omega + \Omega_\Lambda \approx 1$ for $z < 1$ and still remains close to unity up to $z = 2$. This means out to $z \approx 2$ the universe is quasi-Euclidean. Furthermore from (28) it follows that as the universe expands the total density tends to the vacuum energy density $\Omega_\Lambda \rightarrow 1$ (since $\Omega_m \rightarrow 0$). This means a totally 3D spatially flat universe in a totally relaxed state.

Table I shows the two models compared with $\Omega_m =$

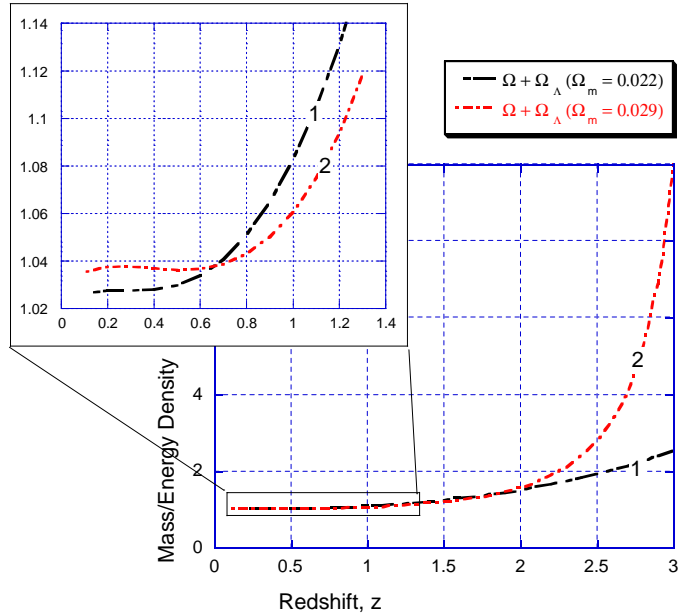


FIG. 7: (Color online) Total mass/energy density $\Omega_\Lambda + \Omega$ as a function of redshift z for the two models. Curve 1 (black) is $\Omega_\Lambda + \Omega$ for the flat *spacevelocity* model with $\Omega_m = 0.022$. Curve 2 (red) is $\Omega_\Lambda + \Omega$ for the curved *spacevelocity* model with $\Omega_m = 0.029$

TABLE I: Mass and energy fractions at a redshift of $z = 1$ for flat and curved models and various values of Ω_m

Density	flat	curved	flat	curved	flat	curved
Ω_m	0.02	0.02	0.03	0.03	0.04	0.04
Ω_Λ	0.905	0.899	0.914	0.905	0.922	0.912
Ω	0.16	0.104	0.24	0.162	0.32	0.225
$\Omega + \Omega_\Lambda$	1.065	1.003	1.154	1.067	1.242	1.137

0.02, 0.03, 0.04 which are all within the bounds of the measured baryonic matter density at the present epoch ($z \approx 0$). From this paper best fits from the two models (flat with $\Omega_m = 0.02$; curved with $\Omega_m = 0.03$) both result in approximately the same total density $\Omega + \Omega_\Lambda = 1.067$ at $z = 1$.

For small z the total density becomes

$$\Omega + \Omega_\Lambda \approx (1 + \Omega_m) + 3z\Omega_m. \quad (29)$$

It follows from (29) that for $\Omega_m = 0.03$ at $z = 0$ the total density $\Omega_m + \Omega_\Lambda \approx 1.03$. This is consistent with recent WMAP data, which gives $\Omega_m + \Omega_\Lambda = 1.02 \pm 0.02$.

However, it follows from (16) and (29) that the universe will always be open, $\Omega < 1$ as it expands. From figure 7 the total density $\Omega + \Omega_\Lambda$ is always greater than unity and as the universe expands, it asymptotically approaches unity—therefore a spatially flat universe devoid of dark matter.

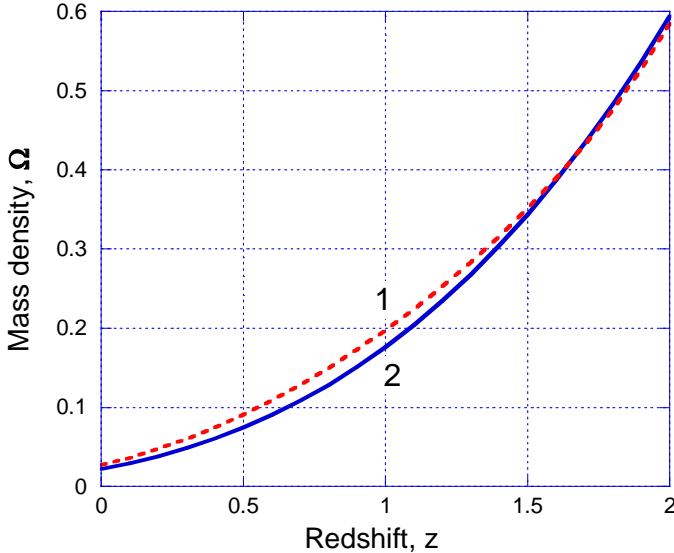


FIG. 8: (Color online) Mass density Ω as a function of redshift z for the two models. Curve 2 (blue solid line) is Ω for the flat *spacevelocity* model with $\Omega_m = 0.022$. Curve 1 (red dashed line) is Ω for the curved *spacevelocity* model derived in the Appendix with $\Omega_m = 0.028$

VIII. CONCLUSION

The 5D brane world of Moshe Carmeli has been applied to the expanding accelerating universe and the magnitude-redshift distance relation has been applied to the distance modulus data from the type Ia SNe measurements up to $z = 1.75$. It has been found that for two models of the dependence of baryonic matter density on redshift the resulting distance-redshift relation fits the data of the high- z supernova teams without the need for dark matter. Also it is shown that the expansion of the universe is speed limited by the usual relativistic Doppler effect.

However the quality of the statistical fits are poor (i.e. large statistical errors) due to the lack of precision in the magnitude-redshift data. It is clearly seen from figures 1, 2 and 4 that there is a large spread in the data. In figure 3 there are only 8 data so the spread is limited.

Considering the range set on the present ($z \approx 0$) baryonic matter density of $0.007 \leq \Omega_b \leq 0.041$ [10] with a best guess of $\Omega_b \approx 0.021$ and the fact that Ω_m must always be > 0 , the best estimates of the (baryonic) matter density for the flat *spacevelocity* model is $\Omega_m = 0.022^{+0.019}_{-0.015}$ and for the curved *spacevelocity* model is $\Omega_m = 0.029^{+0.012}_{-0.022}$.

Models with $\Omega = 1$ are clearly excluded as $\Omega < 1$ for $z < 2$ for both models as shown in figure 6. So too are models with $\Omega_m = 1$ as they cannot in any way be described by the data.

Even though it does not explicitly appear in the Carmeli *spacevelocity* metric, the vacuum energy contribution to gravity, Ω_Λ , is determined from a comparison with the standard model. It is seen that Ω_Λ tends to unity as a function of decreasing redshift. Also since the baryonic matter density $\Omega_m \rightarrow 0$ as the universe expands, the total mass/energy density $\Omega + \Omega_\Lambda \rightarrow 1$. This

indicates that the universe, though always open because $\Omega < 1$, is asymptotically expanding towards a spatially flat state, with a value of $\Omega_\Lambda + \Omega_m \approx 1.029$.

APPENDIX

This appendix deals with a more rigorous approach to the effect that curved *spacevelocity* has on matter density as a function of redshift. However this approach results in a transcendental equation, which could not be used in analytical curve-fitting. Nevertheless the analysis here validates the methods used in sections IV, V.

If we start with the z -derivative of Ω from the right-hand side of (16), we get

$$d\Omega = 3\Omega_m(1+z)^2 dz. \quad (\text{A.1})$$

By the chain rule (A.1) can be written as

$$d\Omega = 3\Omega_m(1+z)^2 \frac{dz}{dr} dr. \quad (\text{A.2})$$

In a flat *spacevelocity* where the $\Omega = 1$ and $e^{\xi/2} = 1$ it follows from (23) that $dz/dr = 1/c\tau$. Now using (23), in general,

$$d\Omega = 3\Omega_m(1+z)^2 \frac{e^{\xi/2}}{c\tau} dr \quad (\text{A.3})$$

which when substituting $e^{\xi/2}$ from (11) and (12) becomes,

$$d\Omega = 3\Omega_m \frac{(1+z)^2}{\sqrt{1 + (1-\Omega) \left(\frac{r}{c\tau}\right)^2}} d\left(\frac{r}{c\tau}\right). \quad (\text{A.4})$$

Finally by substituting $r/c\tau = z$, which is the Hubble law to the lowest order in z in the limit of no gravity, we arrive at an expression which is integrable and describes the matter density in the presence of curved *spacevelocity*.

$$d\Omega \approx 3\Omega_m \frac{(1+z)^2}{\sqrt{1 + (1-\Omega)z^2}} dz. \quad (\text{A.5})$$

From (A.5) it is clear we recover (A.1) when $\Omega = 1$. So all that needs to be done is integrate (A.5) to get Ω as a function of z . But it is not simply solved. It appears difficult to separate Ω in the integrand on the right-hand side from z . So assuming that in (A.5) the value of Ω is approximately constant or only slowly changing as a function of z we integrate and impose the boundary conditions that when $\Omega = 1$ and for $z \ll 1$ then $\Omega = \Omega_m(1+z)^3$. To satisfy both conditions in (A.1) the limits of integration must be from -1 to z . That is

$$\Omega \approx 3\Omega_m \int_{-1}^z \frac{(1+z')^2}{\sqrt{1 + (1-\Omega)z'^2}} dz'. \quad (\text{A.6})$$

This results in

$$\Omega \approx \frac{\Omega_m}{2(1-\Omega)^{3/2}} \left[3\sqrt{1-\Omega} \left((4+z)\sqrt{1+(1-\Omega)z^2} - 3\sqrt{2-\Omega} \right) + 3(1-2\Omega) \left(\operatorname{arcsinh}\sqrt{1-\Omega} + \operatorname{arcsinh}(z\sqrt{1-\Omega}) \right) \right], \quad (\text{A.7})$$

from which it may be determined that $\Omega \rightarrow \Omega_m(1+z)^3$ for arbitrary z in the limit where $\Omega \rightarrow 1$.

In the limit where $z \rightarrow 0$, $\Omega \rightarrow \Omega_m(1+z)^3$ where $\Omega \rightarrow 1$ and $\Omega \rightarrow \Omega_m(0.958+3z) \approx \Omega_m(1+z)^3$ where $\Omega \rightarrow 0$. It is expected that the mass density can always be approximated to yield Euclidean space locally. From the former, the boundary conditions are almost met and hence the approximation is reasonably valid.

The solution to (A.7) is not analytical and must be solved numerically. The form of the transcendental equation does not lend itself to curve fitting as has been done in sections IV, V. However, using the software package Mathematica, it is possible to create a function that is the solution to such an equation as (A.7). This was done and compared with the flat *spacevelocity* model. The result was almost identical to (16) for redshift $z \leq 2$ –

that is, when $\Omega_m = 0.022$ in the flat *spacevelocity* model, $\Omega_m = 0.028$ in the resulting curved *spacevelocity* model. See figure 8 where the density Ω has been plotted for both models up to $z = 2$.

This then confirms the results of the approximate curved *spacevelocity* model used in the main text. Only above $z = 2$ does the curve derived from (A.7) depart from the flat space model of (16). Also for $z \gg 2$ the assumption, that Ω be at most a slowly changing function, breaks down and thus the integration in (A.6) is invalid.

At these higher redshifts the unapproximated form of (A.4) must be solved where $r/c\tau$ is substituted from (15) and $v/c \rightarrow \varsigma = ((1+z)^2 - 1)/((1+z)^2 + 1)$. But that is beyond the scope of this paper.

- [1] Behar, S., Carmeli, M. (2000). *Int. J. Theor. Phys.* **39** (5): 1375-1396
- [2] Burbidge, E.M., Burbidge, G., Fowler, W.A., and Hoyle, F. (1957) *Rev. Mod. Phys.* **29** (4): 547-650
- [3] Burbidge, G. , Hoyle, F. (1998). *Ap. J.* **509** (Dec): L1-L3
- [4] Carmeli, M. (1996). *Commun. Theor. Phys.* **5**:159
- [5] Carmeli, M. (1998). *Int. J. Theor. Phys.* **37** (10): 2621-2625
- [6] Carmeli, M. (2002). *Cosmological Special Relativity*. Singapore, World Scientific
- [7] Carmeli, M. (2002). arXiv: astro-ph/0205396 v4 2 Jun 2002
- [8] Freedman, W.L., *et al.* (1994). *Nature* **371**(Oct): 757-762
- [9] Freedman, W.L., *et al.* (2000). Talk given at the 20th Texas Symposium on Relativistic Astrophysics, Austin, Texas 10-15 December 2000. arXiv:astro-ph/0012376 v1 18 Dec 2000
- [10] Fukugita, M., Hogan, C.J., and Peebles, P.J.E. (1998). *Ap. J.* **503** (Aug): 518-530
- [11] Garnavich, P.M., *et al.* (1997). *Bulletin of the American Astronomical Society* **29** (7): 1350
- [12] Hartnett, J.G. (2004). *Int. J. Theor. Phys.* in press, arXiv:gr-qc/0407082
- [13] Hartnett, J.G. (2004). *Int. J. Theor. Phys.* in press, arXiv:gr-qc/0407083
- [14] Knop, R.A., *et al* (2003). *Ap. J.* **598** (Nov): 102-137
- [15] Krauss, M.K. (1998). *Ap. J.* **501** (July): 461-466
- [16] Ostriker, J.P., Steinhardt, P.J. (1995). *Nature* **377** (Oct): 600-602
- [17] Perlmutter, S., *et al.* (1997). *Bulletin of the American Astronomical Society* **29** (5): 1351
- [18] Riess, A.G., Press, W.H. and Kirshner, R.P. (1995). *Ap. J.* **438** (Jan): L17-L20
- [19] Riess, A.G., *et al.* (1998). *Astron. J.* **116** (Sept): 1009-1038
- [20] Riess, A.G., *et al.* (2004). *Ap. J.* **607** (June): 665-687
- [21] Tonry, L.R., *et al* (2003). *Ap. J.* **594** (Sep): 1-24
- [22] White, S.D., Navarro, J.F., Evrard, A.E. and Frenk, C.S. (1993). *Nature* **366**(Dec): 429-433
- [23] Wright, A.E., Disney, M.J., and Thomson, R.C. (1990). *Proc. ASA* **8** (4): 334-338